Optical Negative Refraction in Ferrofluids with Magnetocontrollability

Y. Gao,[1,2] J. P. Huang,[1,*] Y. M. Liu,[3] L. Gao,[4] K. W. Yu,[2] and X. Zhang[3]

[1]*Department of Physics and Surface Physics Laboratory (National Key Laboratory), Fudan University, Shanghai 200433, China*
[2]*Department of Physics and Institute of Theoretical Physics, The Chinese University of Hong Kong,*
Shatin, New Territories, Hong Kong
[3]*NSF Nanoscale Science and Engineering Center (NSEC), 5130 Etcheverry Hall, University of California,*
Berkeley, California 94720-1740, USA
[4]*Department of Physics, Soochow University, Suzhou 215006, China*
(Received 5 October 2009; published 20 January 2010)

We numerically demonstrate optical negative refraction in ferrofluids containing isotropic Fe_3O_4 nanoparticles, each having an isotropic Ag shell, in the presence of an external dc magnetic field H. The all-angle broadband optical negative refraction with magnetocontrollability arises from H-induced chains or columns. They result in hyperbolic equifrequency contour for transverse magnetic waves propagating in the system. The finite element simulations verify the analyses using the effective medium approximation. Experimental demonstration and potential applications are suggested and discussed.

In 1968, Veselago [1] theoretically investigated the electrodynamic consequences of a medium with simultaneously negative permittivity and permeability. He predicted that such a medium possesses a negative (phase) index, which can result in a reversed Snell's law, i.e., negative refraction. People have realized negative refraction of optical waves or microwaves in different systems, including metamaterials [2,3], photonic crystals [4], plasmonic waveguides [5], chiral media [6], and superconductor-ferromagnet superlattices [7]. The significant application of negative refraction is the concept of a perfect lens, which can lead to subwavelength imaging beyond the diffraction limit [8].

However, almost all the existing methods for achieving negative refraction were proposed or established in the realm of solid materials, in contrast to soft materials with the specific characteristic "softness". Literally softness might offer an extra freedom of tailoring physical properties; hence, it encourages us to investigate optical refraction in certain soft materials. As a result, we reveal, for the first time, a new class of all-angle broadband optical negative refraction in ferrofluids with magnetocontrollability. Its underlying mechanism arises from assembly metallic chain or column structures induced by an external dc magnetic field H. This work paves a new way for designing tunable, active metamaterials.

In general, ferrofluids are colloidal suspensions composed of ferromagnetic or ferrimagnetic nanoparticles of about 10 nm diameter dispersed in a carrier fluid, usually water or kerosene [9]. Two typical kinds of materials for fabricating such nanoparticles are Co and Fe_3O_4 [9]. In this work we shall consider an aqueous ferrofluid system which contains spherical isotropic Fe_3O_4 nanoparticles, each coated with a spherical isotropic Ag shell, in the presence of H in z axis. The reason why we choose Fe_3O_4 rather

than Co is due to its lower optical absorption. In principle, the Ag used for making shells may be replaced by other metallic materials having a permittivity with a big negative real part and small positive imaginary part. If water is replaced with kerosene, the qualitative results as to be revealed would remain unchanged. Both experiments [10–12] and computer simulations [13,14] have shown that nanoparticle chains can be formed in ferrofluids as the magnetic dipolar interaction overwhelms the thermal energy. For ferrofluids, the field-induced columnar phase with equal spacing was experimentally reported [11,12] in confined ferrofluid films subjected to an in-plane H, and the dipolar interaction between the chains (which are locally displaced in a hexagonal fashion) gives rise to their arrangement in columns. In other words, nanoparticles in ferrofluids can exist in the form of both (either) chains and (or) columns. In our work, the word "*chain*" denotes a single-particle-width z-directed array of touching Fe_3O_4 nanoparticles with an Ag shell, and "*column*" represents the aggregation of such chains, namely, the chains aggregate together to form z-directed thick columns. Incidentally, throughout this work both permittivities and permeabilities denote relative ones.

An effective medium approximation and a 2D finite element method.—Let us start by considering the ferrofluid system containing Fe_3O_4 nanoparticles coated by an Ag shell, in the presence of z-directed H. The chains, each having the same number n of nanoparticles [15], are induced to appear by H. They are all directed along z axis, and are assumed to be randomly suspended in the system. In the quasistatic approximation, we can utilize the anisotropic form of the effective medium approximation (EMA) [16] to calculate the effective permittivity tensor with three nonzero diagonal components ε_{xx}, $\varepsilon_{yy}(= \varepsilon_{xx})$, and ε_{zz} given by

$$p \frac{\varepsilon_1 - \varepsilon_{xx,zz}}{\varepsilon_1 + (\frac{1}{g_{x,z}} - 1)\varepsilon_{xx,zz}} + (1 - p) \frac{\varepsilon_2 - \varepsilon_{xx,zz}}{\varepsilon_2 + (\frac{1}{g_{x,z}} - 1)\varepsilon_{xx,zz}} = 0,$$

$$(1)$$

where p is the volume fraction of the coated nanoparticles, and ε_2 the permittivity of water. Except for the EMA, some other theories which appear to be more complex can also be adopted, e.g., the spectral representation approach [16,17]. For Eq. (1) we have modeled an individual chain as a spheroid with g_x (shape factor perpendicular to H) and g_z (shape factor along H) [18]. They satisfy a geometrical sum rule $g_z + 2g_x = 1$ [19]. It is important to note that the result calculated by the isotropic counterpart of the EMA, namely, Eq. (1) with $g_{x,z} = 1/3$, was demonstrated to reasonably lie in the Hashin-Shtrikman bounds which provide the tightest constraints for the effective permittivity of a composite comprising an isotropic mixture of two isotropic dielectric materials [20]. Thus in view of the physical reasonability and formal compactness, we prefer to use the EMA [Eq. (1)] for treating the ferrofluid system. In Eq. (1) ε_1 denotes the equivalent permittivity of the coated nanoparticle. It can be given by solving Laplace's equation of electrostatics together with appropriate boundary conditions [21], which is valid in our quasistatic system where the incident wavelength λ is much larger than the size of the coated nanoparticles. After some straightforward derivations, we obtain

$$\varepsilon_1 = \varepsilon_a \frac{\varepsilon_f(1 + 2\rho) + 2\varepsilon_a(1 - \rho)}{\varepsilon_f(1 - \rho) + \varepsilon_a(2 + \rho)} \qquad (2)$$

with $\rho = r^3/(r + d)^3$, where r is the radius of the core (Fe$_3$O$_4$) with permittivity ε_f, and d is the thickness of the shell (Ag) with permittivity ε_a. Equation (2) is an exact solution for an isolated Fe$_3$O$_4$ nanoparticle with an Ag shell, but it serves as the result of the first-order approximation for such a nanoparticle in our ferrofluid system by neglecting local field effects caused by all the other nanoparticles. In Eq. (1), g_z is given by a simple approximation $g_z = 1/(1 - n^2) + n \ln(n + \sqrt{n^2 - 1})/(n^2 - 1)^{3/2}$ [22], where $n \geq 2$. In reality, n is proportional to the ratio of magnetic energy to thermal energy (a lowest-order assumption). Thus, without loss of generality, n will be used to equivalently represent the strength of H. This correlation corresponds to the fact that higher H yields larger n [13]. Apparently $H = 0$ causes $n = 1$ or $g_z = 1/3$. In this case, the nanoparticles are randomly suspended in the ferrofluid system, resulting in an isotropic effective permittivity. It is worth noting that the EMA [Eq. (1)] has included energy dissipation related to absorption. On the other hand, the effect of scattering is assumed to be neglected due to the small scattering cross section of a chain with respect to an incident wavelength.

We use the software COMSOL Multiphysics 3.5 to perform finite element simulations of optical refraction in ferrofluids, see Fig. 1. A transverse magnetic (TM) Gaussian beam with a width of 1.6 μm in xz plane with
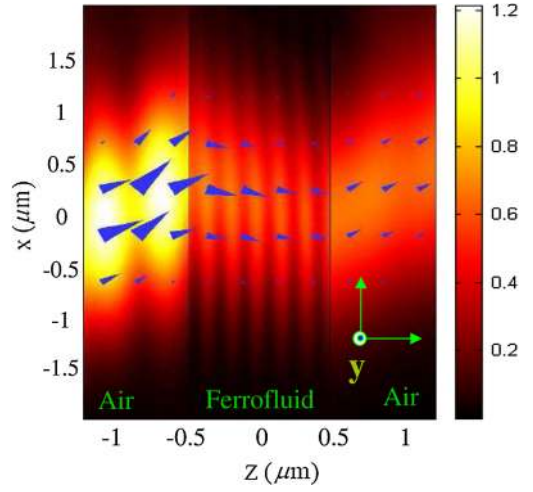

FIG. 1 (color online). 2D finite element simulations of the distribution of the absolute value (denoted by the color or brightness) of electric field components of an incident TM wave with $\lambda = 758$ nm, in a ferrofluid system of thickness 1 μm containing chains of Fe$_3$O$_4$ nanoparticles coated by an Ag shell. The ferrofluid system is replaced by an effective medium described by the parameters calculated according to Eq. (1). The direction and size of the blue or dark arrows indicate, respectively, the direction and magnitude of the local power flow or Poynting vector.

a y-directed magnetic field component is incident to the ferrofluid system at an angle $\phi = 30°$ with respect to z axis. Here ϕ just denotes the angle of incidence. Using Eq. (1), we obtain $\varepsilon_{xx} = 4.43 + 0.15i$ and $\varepsilon_{zz} = -3.29 + 0.19i$ according to the parameters: $\varepsilon_1 = -21.4 + 0.9i$, $\varepsilon_2 = 1.77$, $p = 0.22$, $n = 50$, and the length of each chain is 1 μm. Here ε_1 has been calculated according to Eq. (2) with the parameters: $r = 5$ nm, $d = 5$ nm, $\varepsilon_f = 4.8 + 2.2i$ (as experimentally measured at $\lambda = 758$ nm for magnetite, a ferrimagnet and crystallites with the inverse cubic spinel structure [23]), and $\varepsilon_a = -20.61 + 1.27i$ (which was measured for a Ag thin film at $\lambda = 758$ nm [24]). Note we already take into account the conductivity property of the materials by using the complex permittivity values since the conductivity and permittivity are related [25]. Figure 1 plots the distribution of the absolute value of electric field components, and it clearly demonstrates the appearance of negative refraction.

To understand the finite element simulation results depicted in Fig. 1, we resort to a theoretical approach for the system with $\mathrm{Re}(\varepsilon_{zz}) < 0$ and $\mathrm{Re}(\varepsilon_{xx,yy}) > 0$. Here $\mathrm{Re}(\cdots)$ means the real part of $\cdots$. On the basis of Maxwell's equations, for the TM waves with the magnetic field component polarized in the y axis and the electric field component located in the xz plane, the dispersion relation for the wave propagating in a general anisotropic medium is

$$(k_x^2/\varepsilon_{zz}) + (k_z^2/\varepsilon_{xx}) = \mu_{yy}k_0^2, \qquad (3)$$

where k_x (or k_z) is the x (or z) component of wave vector **k**, and $k_0 = 2\pi/\lambda$ the wave number in free space. Clearly, the

permittivity tensor terms (ε_{xx} and ε_{zz}) and the permeability tensor term (μ_{yy}) are involved due to the TM polarization. At optical frequencies, the permeability of natural materials can be taken to unity [19], and therefore the effective permeability of the ferrofluid system is about unity. So the value of μ_{yy} is taken as unity in Eq. (3) and the following analyses. Negative refraction can be realized in the ferrofluid system because of the hyperbolic equifrequency surface and the boundary condition for electromagnetic waves at the interface between a uniaxial medium and an isotropic medium [26]. One might resort to Maxwell's equations to calculate the Poynting vector directly. The x and z components of the time-averaged Poynting vector $\mathbf{S}$ are, respectively, given by [27]

$$S_x = \frac{k_x}{\varepsilon_{zz}} \frac{H_y^2}{2\omega\varepsilon_0} \quad \text{and} \quad S_z = \frac{k_z}{\varepsilon_{xx}} \frac{H_y^2}{2\omega\varepsilon_0}. \quad (4)$$

Then the angles of refraction for the wave vector $\mathbf{k}$ and Poynting vector $\mathbf{S}$ are, respectively, given by

$$\theta_k = \tan^{-1}(k_x/k_z), \quad (5)$$

$$\theta_s = \tan^{-1}(S_x/S_z) = \tan^{-1}[k_x\varepsilon_{xx}/(k_z\varepsilon_{zz})]. \quad (6)$$

For the system with $\text{Re}(\varepsilon_{zz}) < 0$ and $\text{Re}(\varepsilon_{xx}) > 0$, there exists positive refraction for $\mathbf{k}$, because of the hyperbolic equifrequency contour, the conservation of the tangential wave vector, and the causality theorem [27]. On the basis of Eqs. (3) and (6), the effective refractive index

$$\eta = \sin\phi/\sin\theta_s \quad (7)$$

can be computed. When $\text{Re}(\varepsilon_{zz}) < 0$ and $\text{Re}(\varepsilon_{xx}) > 0$, Eq. (6) [or Eq. (7)] can yield $\text{Re}(\theta_s) < 0$ [or $\text{Re}(\eta) < 0$], namely, negative refraction for the Poynting vector, as shown in Fig. 1.

A 3D finite element method beyond the EMA.—In the above analyses, we use the EMA [Eq. (1)] to calculate the effective permittivity of the ferrofluid system containing chains. As a result, negative refraction has been revealed. Experimental results [11,12] demonstrated that there exist columns with equal spacing in confined ferrofluid films in the presence of an in-plane H. Accordingly, we deduce that there also exist such columns with equal spacing in the ferrofluid system of our interest. This should be a reasonable deduction because similar to the confined ferrofluid films, our system possesses the same dipolar interaction between (locally displaced) chains that creates columns. In order to show the validity of the above analyses using the EMA, we conduct 3D finite element simulations for a ferrofluid system containing columns with equal spacing. Certainly if we investigate the same system with chains rather than columns, in principle the present 3D simulations would work the same. However, they are quite time-consuming. For the comparison with Fig. 1 (2D simulations), in Fig. 2 we also take $\varepsilon_2 = 1.77$ and the volume fraction of the columns $p = 0.22$. Each column has a length of 1.0 μm and a permittivity of $\varepsilon_1 = -21.4 +$
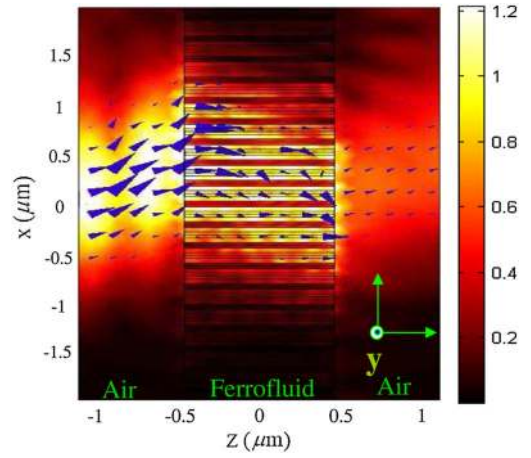

FIG. 2 (color online). Cross-sectional view of 3D finite element simulations of the distribution of the absolute value of electric field components of an incident TM wave with $\lambda = 758$ nm, in a ferrofluid system of thickness 1 μm containing columns aggregated by chains of Fe_3O_4 nanoparticles coated by an Ag shell. For convenience we replace each column with a solid cylinder by assuming the solid cylinder to possess the same electromagnetic responses as the column. This assumption is reasonable, at least to some extent, since the incident wavelength is much larger than the size of coated nanoparticles. We set the cross sections of the cylinders to exist in a hexagonal lattice since equal spacing between columns was experimentally observed [11]. The radius of the cylinder is 30 nm, and the center-to-center separation between two adjacent cylinders is 122 nm.

$0.9i$. Also, a TM Gaussian beam with a width of 1.6 μm is incident at $\phi = 30°$. Figure 2 shows the result simulated by the 3D finite element method based on the software COMSOL Multiphysics 3.5. It clearly demonstrates the appearance of optical negative refraction, which echoes with Fig. 1. The excellent agreement is expected, since the EMA is valid considering the size and spacing of nanoparticles are much smaller than the wavelength λ. The local periodic structures of the chains or columns will not significantly influence the optical property, but can be incorporated as a high-order approximation based on the Ewald-Kornfeld formulation [16].

Numerical results.—The agreement between Fig. 1 and 2 gives us confidence to further investigate the optical properties of the ferrofluid system by using the EMA. Figure 3 shows the real part of η as a function of n, p, and ϕ at $\lambda = 758$ nm. It is worth reminding that higher H leads to larger n. Evidently high H together with suitable p can lead to negative refraction, $\text{Re}(\eta) < 0$. Namely, one can achieve the transition from positive refraction to negative refraction for the Poynting vector by tuning H and/or p. Further the negative refraction $\text{Re}(\eta) < 0$ is shown to exist within the full range of ϕ (namely, all-angle negative refraction). Figure 4 displays the imaginary part of η, namely *extinction coefficient* (which is proportional to optical absorption). We find it varies with respect to H, p, and/or ϕ. In other words, one is allowed to achieve low optical absorption by choosing H, p, and ϕ appropriately.
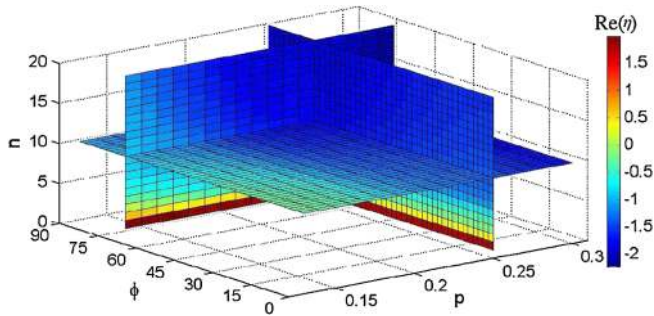
FIG. 3 (color online).   Real part of the effective refractive index
Re(η) calculated according to Eq. (7) as a function of n, p, and
ϕ (degree) at $\lambda = 758$ nm. Three cross sections correspond to
$n = 10$, $p = 0.25$, and $\phi = 70°$, respectively.

We also confirmed that (all-angle) broadband negative
refraction can be achieved in such a ferrofluid system by
investigating two other incident wavelengths $\lambda = 661$ nm
and 706 nm at $n = 50$ and $p = 0.22$ (no figures shown
herein). For the calculations, we adopted the experimental
data: $\varepsilon_a = -20.09 + 0.45i$ [24] and $\varepsilon_f = 4.8 + 2.8i$ [23]
at $\lambda = 661$ nm, and $\varepsilon_a = -23.40 + 0.39i$ [24] and $\varepsilon_f =
5.0 + 2.4i$ [23] at $\lambda = 706$ nm. Clearly, the wavelength
bandwidth can be wider for the system.

In summary, for the first time, we have demonstrated
that magneto controllable all-angle broadband negative
refraction at optical frequencies can be realized in aqueous
ferrofluids, which are made of Fe_3O_4 nanoparticles coated
by an Ag shell. In looking for experimental realization, the
most important point is that the ratio between magnetic
energy and thermal energy must be high enough, which
causes the formation of chains and/or columns. Since the
permanent magnetic moment of Fe_3O_4 nanoparticles is
about $2.4 \times 10^4 \mu_B$ [9] (μ_B: the Bohr magneton), we can
estimate the threshold magnetic field 14.8 kA/m above
which the corresponding magnetic energy can overwhelm
the thermal energy $1/40$ eV at room temperature so as to
obtain appreciable H-induced formation of chains/col-
umns. Practically one might choose a higher H together
with a lower temperature. On the other hand, the system at
zero field ($H = 0$) may be stabilized against agglomeration
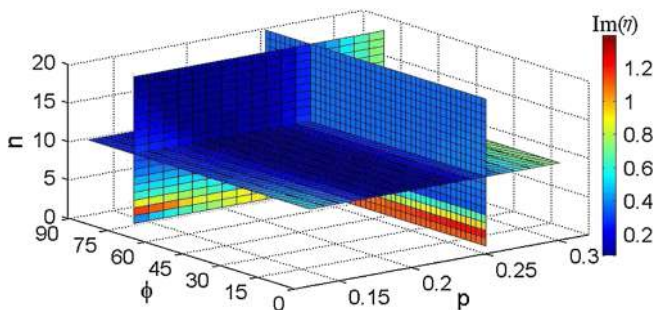by coating nanoparticles with long polymer molecules

(sterically) or decorating them with charged groups (elec-
trostatically). The magnetocontrollable negative refraction
in ferrofluids presented here promises a new regime and a
number of potential applications of metamaterials. The
field-induced-assembly system of nanoparticles may real-
ize a large specimen which is difficult to fabricate using
top-down techniques. Moreover, we can engineer the spa-
tial dielectric constant by the external magnetic fields for
reconfigurable optical devices, such as lenses [27], invis-
ible cloaks [28], and waveguides.

*jphuang@fudan.edu.cn
 [1] V. G. Veselago, Sov. Phys. Usp. **10**, 509 (1968).
 [2] R. A. Shelby et al., Science **292**, 77 (2001).
 [3] J. Yao et al., Science **321**, 930 (2008).
 [4] E. Cubukcu et al., Nature (London) **423**, 604 (2003).
 [5] H. Shin and S. H. Fan, Phys. Rev. Lett. **96**, 073907 (2006).
 [6] J. B. Pendry, Science **306**, 1353 (2004).
 [7] A. Pimenov et al., Phys. Rev. Lett. **95**, 247009 (2005).
 [8] J. B. Pendry, Phys. Rev. Lett. **85**, 3966 (2000).
 [9] S. Odenbach, Magnetoviscous Effects in Ferrofluids
     (Springer, Berlin, 2002).
[10] K. Butter et al., Nature Mater. **2**, 88 (2003).
[11] M. Klokkenburg et al., Phys. Rev. Lett. **97**, 185702 (2006).
[12] M. Klokkenburg et al., Phys. Rev. E **75**, 051408 (2007).
[13] Z. W. Wang et al., Phys. Rev. E **66**, 021405 (2002).
[14] R. A. Trasca and S. H. L. Klapp, J. Chem. Phys. **129**,
     084702 (2008).
[15] If the chains have different n, a volume average may be
     adopted for Eq. (1) instead.
[16] J. P. Huang and K. W. Yu, Phys. Rep. **431**, 87 (2006).
[17] D. J. Bergman, Phys. Rep. **43**, 377 (1978).
[18] The shape factors are the same as depolarization or
     demagnetization factors for spheroids.
[19] L. D. Landau, E. M. Lifshitz, and L. P. Pitaevskii, Electro-
     dynamics of Continuous Media (Pergamon, New York,
     1984), 2nd ed.
[20] D. J. Bergman and D. Stroud, Solid State Phys. **46**, 147
     (1992).
[21] T. B. Jones, Electromechanics of Particles (Cambridge
     University Press, Cambridge, England, 1995).
[22] C. Z. Fan and J. P. Huang, Appl. Phys. Lett. **89**, 141906
     (2006).
[23] A. Schlegel et al., J. Phys. C **12**, 1157 (1979).
[24] P. B. Johnson and R. W. Christy, Phys. Rev. B **6**, 4370
     (1972).
[25] J. D. Jackson, Classical Electrodynamics (John Wiley &
     Sons, New York, 2001), 3rd ed.
[26] P. A. Belov, Microwave Opt. Technol. Lett. **37**, 259
     (2003).
[27] Y. M. Liu et al., Opt. Express **16**, 15439 (2008).
[28] J. B. Pendry et al., Science **312**, 1780 (2006).

FIG. 4 (color online).   Same as Fig. 3, but for imaginary part of
the effective refractive index Im(η).